

Design and synthesis of benzimidazole phenol-porphyrin dyads for the study of bioinspired photoinduced proton-coupled electron transfer

S. Jimena Mora^{*a}, Daniel A. Heredia^b, Emmanuel Odella^a, Uma Vrudhula^a,
Devens Gust[∅], Thomas A. Moore^a and Ana L. Moore^{*a}

^aSchool of Molecular Sciences, Arizona State University, Tempe, Arizona 85287, USA

^bDepartamento de Química, Facultad de Ciencias Exactas, Físico-Químicas y Naturales, Universidad Nacional de Río Cuarto, Agencia Postal Nro 3, 5800 Río Cuarto, Córdoba, Argentina

This paper is part of the 2019 Women in Porphyrin Science special issue.

Received 21 July 2019

Accepted 10 August 2019

ABSTRACT: Benzimidazole phenol-porphyrin dyads have been synthesized to study proton-coupled electron transfer (PCET) reactions induced by photoexcitation. High-potential porphyrins have been chosen to model P680, the photoactive chlorophyll cluster of photosynthetic photosystem II (PSII). They have either two or three pentafluorophenyl groups at the *meso* positions to impart the high redox potential. The benzimidazole phenol (BIP) moiety models the Tyr_z-His190 pair of PSII, which is a redox mediator that shuttles electrons from the water oxidation catalyst to P680^{•+}. The dyads consisting of a porphyrin and an unsubstituted BIP are designed to study one-electron one-proton transfer (E1PT) processes upon excitation of the porphyrin. When the BIP moiety is substituted with proton-accepting groups such as imines, one-electron two-proton transfer (E2PT) processes are expected to take place upon oxidation of the phenol by the excited state of the porphyrin. The *bis*-pentafluorophenyl porphyrins linked to BIPs provide platforms for introducing a variety of electron-accepting moieties and/or anchoring groups to attach semiconductor nanoparticles to the macrocycle. The triads thus formed will serve to study the PCET process involving the BIPs when the oxidation of the phenol is achieved by the photochemically produced radical cation of the porphyrin.

KEYWORDS: proton-coupled electron transfer (PCET), photosystem II, pentafluorophenyl porphyrin, benzimidazole derivatives.

INTRODUCTION

The photosynthetic process starts with the capture of solar energy by pigment-protein and in some cases pigment-pigment complexes known as antennas wherein the electromagnetic energy of light is converted into the chemical potential energy of a molecular excited

state. This singlet excitation energy is then transferred to a membrane-protein complex known as a reaction center (RC), where it is further transformed by charge separation into chemical redox potential. Photosystem II (PSII) is the RC of plants, cyanobacteria and algae, where multistep electron transfer processes produce reduced quinones and molecular oxygen from water splitting [1–3].

The primary electron donor in PSII is a chlorophyll cluster denominated P680. Its excited state initiates the multistep electron transfer forming P680^{•+} and a reduced quinone Q^{•-}. The high potential of P680^{•+} (~1.3 V vs. NHE [4]) is required to oxidize the oxygen-evolving

[∅]SPP full member in good standing

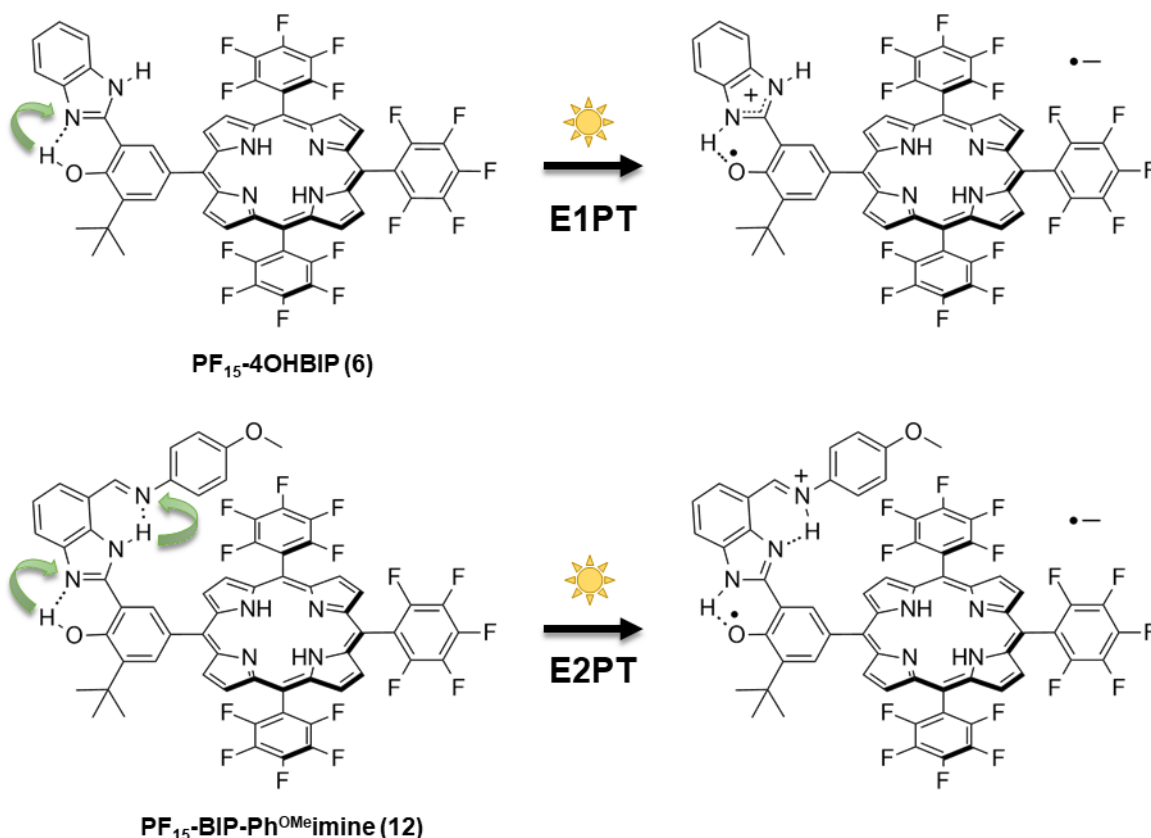
*Correspondence to: School of Molecular Sciences, Arizona State University, 1711 S. Rural Rd, Tempe, Arizona 85287-1604, United States, fax: (480) 965 274, S. Jimena Mora, email: smora2@asu.edu; Ana L. Moore, email: amoore@asu.edu.

complex (OEC), the catalytic site where water oxidation takes place. The oxidation of the OEC by P680⁺ takes place *via* a redox-mediating tyrosine (Tyr_z). The phenolic proton of this residue is hydrogen bonded to the nitrogen lone pair of the imidazole of nearby His190. Oxidation of Tyr_z by P680⁺ is accompanied by proton transfer to His190 [4, 5]. This reaction is one of the best known proton-coupled electron transfer (PCET) processes occurring in nature [6–8]. Protons derived from water splitting are transferred into the thylakoid lumen, contributing to the generation of proton motive force (PMF), which drives myriad bioenergetic processes including the synthesis of ATP from ADP and inorganic phosphate [7, 9].

As was previously reported, benzimidazole phenol (BIP) and its substituted derivatives can be used as models of the redox mediating Tyr_z-His190 pair [10–13]. Evidence of a strong H-bond between the phenol (model of Tyr_z) and the lone pair of the nitrogen of benzimidazole (model of His190) comes from ¹H NMR and FT-IR studies of these constructs [10]. Also, electrochemical measurements show that the oxidized phenol in some of the constructs is thermodynamically capable of activating water oxidizing catalysts. The BIP itself, which lacks substitution on the benzimidazole ring, is known to undergo proton transfer from the phenol to the nitrogen of the

imidazole upon one-electron oxidation of the phenol. This is an example of an E1PT reaction (one-electron, one-proton) [10, 14].

By adding specific substitutions at the 7-position of the benzimidazole (see Scheme 1), BIP becomes capable of two proton transfers upon the oxidation of the phenol (an E2PT process) [10, 15]. When the benzimidazole is substituted with amines the second proton transfer is observed, but the phenoxyl radical/phenol redox potential decreases by ~300 mV compared to that of the BIP lacking substitution on the benzimidazole ring. Therefore, amino-substituted BIP constructs cannot be used as relays in water oxidizing schemes, due to insufficient driving force for the oxidation of the water oxidizing catalyst. On the other hand, some imine-substituted BIPs are able to maintain the high potential of the phenoxyl radical/phenol couple even after the second proton transfer occurs. In general, in this genre of PCET processes proton transfer takes place across hydrogen bonded partners and the driving force for a proton transfer can be affected by interrelated factors such as the ΔpK_a and the H-bond strength between the two partners. For example, substituents at the *para*-position of an *N*-phenylimine moiety can affect the ratio of E1PT to E2PT products. Strong electron withdrawing groups such as -CN and -CF₃ decrease the imine nitrogen basicity and the H-bond strength, leading to a large percentage of the



Scheme 1. PCET processes in dyads consisting of porphyrins covalently attached to benzimidazole phenol derivatives

E1PT product. Additionally, strong electron donating groups like $-OCH_3$ increase the basicity of the imine nitrogen and the H-bond strength, generating only the E2PT product, as was found with the amino-substituted BIPs. In these cases the proton translocation distance across the H-bond network is about 6 Å [15].

The synthetic availability of porphyrins, and in particular high-potential fluorinated porphyrins [13, 16], has allowed the construction of quite elaborate structures containing porphyrins as building blocks. For example, three covalently linked redox subunits in a triad composed of a BIP moiety, a porphyrin and a semiconductor nanoparticle have been reported. In this system, the nanoparticle of TiO_2 or SnO_2 accepts an electron from the photoexcited porphyrin yielding the porphyrin radical cation, which in turn can oxidize the BIP creating a long-lived charge-separated species [17–20].

In this work, we present the synthetic routes for a series of porphyrins attached to benzimidazole phenol derivatives that mimic some of the aspects of the function of P680-Tyr_z-His190 components of PSII (Scheme 1). These synthetic constructs can undergo single or double proton transfers upon oxidation of the phenol. Both electron and proton transfer can be followed by infrared spectroelectrochemistry (IRSEC) because the protonation sites can be readily identified by the appearance of well-established changes in the IR spectra as a consequence of the bonding changes occurring during the oxidation of the phenol and reduction of the porphyrin. In future studies these constructs will be used to characterize the dynamics of E1PT and E2PT processes initiated by the excited state of the porphyrin.

RESULTS AND DISCUSSION

Design and synthesis

The formation of the asymmetric porphyrins was carried out using Lindsey's method [21, 22], by condensation of 5-(pentafluorophenyl)dipyrromethane (F_5 -DPM) and combinations of the corresponding aldehydes shown in Chart 1. The reaction was carried out in $CHCl_3/0.75\%$ EtOH and was catalyzed by boron-trifluoride etherate (BF_3OEt_2). After oxidation with 2,3-dichloro-5,6-dicyano-1,4-benzoquinone (DDQ), the desired porphyrins were obtained in reasonably good yield. The hydroxy group is at the *para* and *ortho* position in compounds **2** and **3**, respectively. This affects the strength of the H-bond between the OH and the imidazole nitrogen in the isomeric dyads **6** and **7**, which were synthesized from **2** and **3**, respectively, (see below). Study of these systems will establish a correlation between this structural feature and the dynamics of the PCET process. The presence of an aryl iodine or bromine moiety in compounds **4** and **5** will permit the inclusion of additional components such as anchoring groups to attach the dyads to semiconductor nanoparticles or strong electron-accepting units to produce triad systems [18, 19, 23–25].

As shown in Scheme 2, the remaining aldehyde group in each porphyrin was condensed with phenylenediamine or its carbomethoxy derivative by the Philipps–Ladenburg reaction to yield the corresponding BIP-porphyrin derivatives. Compounds **6** and **7** were designed to undergo E1PT processes.

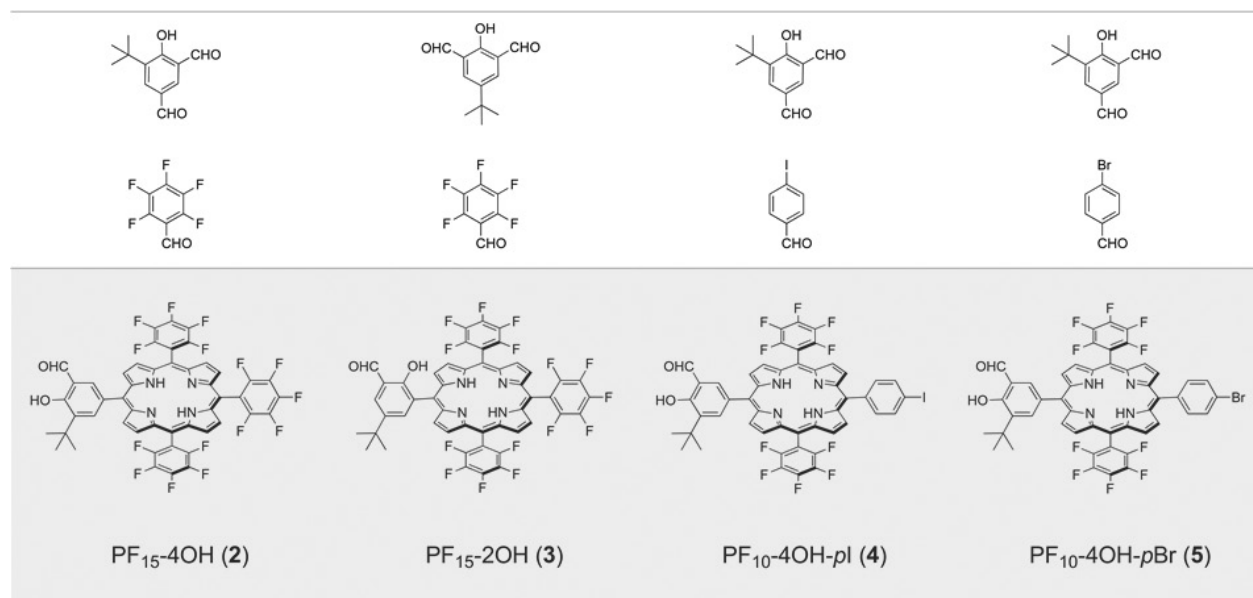
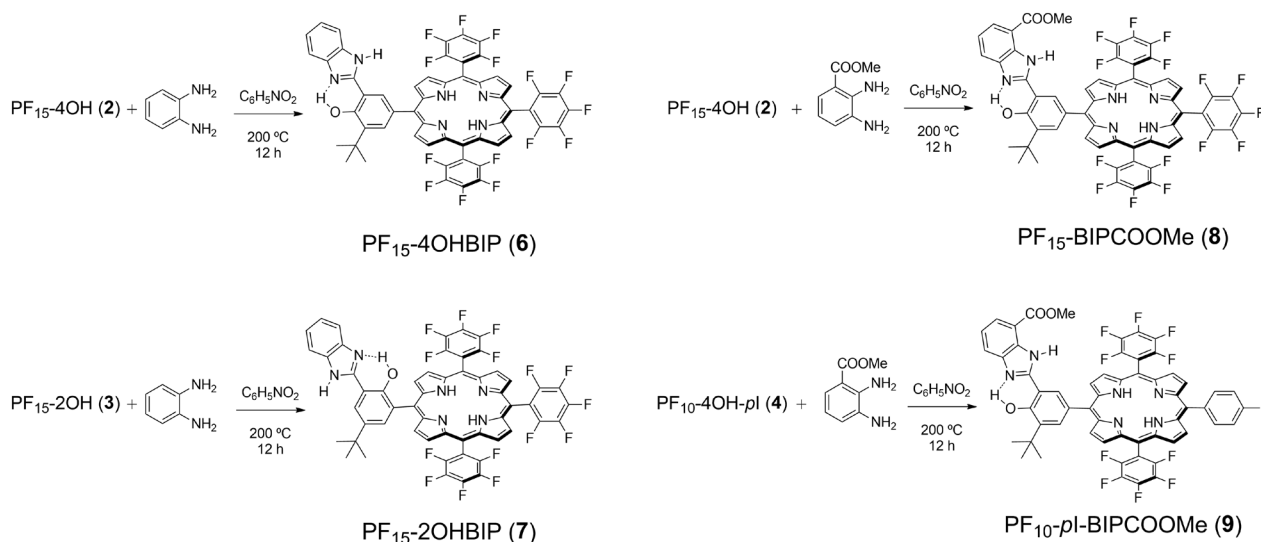
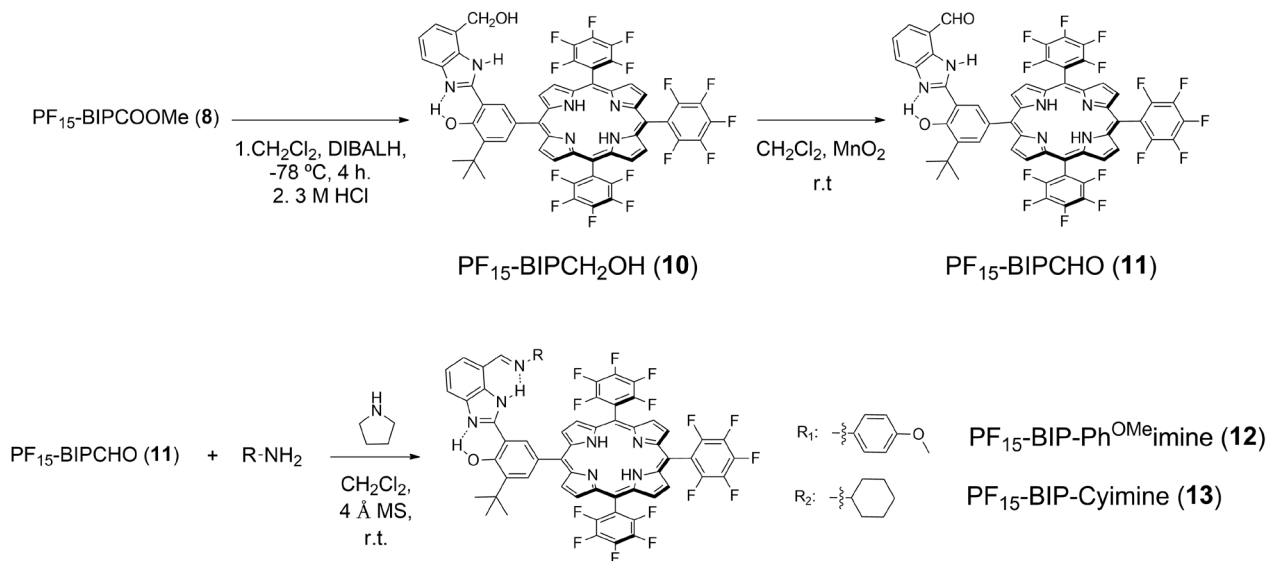


Chart 1. The combination of aldehydes shown in the top panel were mixed with F_5 -DPM (2 equiv.) in $CHCl_3$ at room temperature under argon atmosphere, catalyzed by BF_3OEt_2 (~1 h) and oxidized with DDQ (overnight at 40 °C) to give the corresponding porphyrins shown in the panel below. Secondary products are not shown



Scheme 2. Philips–Ladenburg reactions used in the synthesis of benzimidazoles covalently attached to porphyrins



Scheme 3. Synthetic route to generate porphyrin-BIPCHO, precursor of compounds **12** and **13**. The same procedure was followed starting with porphyrin **9** to obtain PF₁₀-pI-BIPCHO (**15**) (Scheme S1)

The ester group at the 7-position of the benzimidazole attached to the porphyrin (Scheme 2, compounds **8** and **9**), was reduced to the alcohol followed by allylic oxidation to give the corresponding aldehyde **11** (Scheme 3). This reaction was carried out in milder conditions (room temperature) and no overoxidation to carboxylic acid was observed. It is well known that pentafluorophenyl-substituted porphyrins are susceptible to regioselective nucleophilic aromatic substitution reactions (S_NAr) in the presence of amines, thiols, alcohols and other basic compounds, with selective substitution at the *para*-fluoro positions [26]. This situation restricts the reaction conditions that can be used to reduce the ester group. In the present work, the reaction was successfully carried out under mild conditions using diisobutylaluminum

hydride (DIBALH) in dry dichloromethane at -78°C . The aldehyde group in **11** was used to attach the phenyl imine groups, and could be used to introduce a second benzimidazole if so desired. The imino group was incorporated by a general aminocatalytic method [27]. As was previously reported, imines act as a secondary proton acceptor; these systems are designed to undergo E2PT processes while maintaining a higher potential for the phenoxyl radical/phenol redox couple [15]. Because these imines are prone to hydrolysis, compounds **12** and **13** were used without further purification (they hydrolyze on silica gel columns or TLCs). For this reason, the formation of the imine in compound PF₁₀-pI-BIPCHO (**15**) will not be carried out until it is attached to a compatible third structure. As mentioned before, PF₁₀-pI-BIPCHO is a

suitable and versatile building block for the construction of triads. The aryl iodide moiety can be functionalized by cross coupling reactions such as Suzuki, Sonogashira, Heck, Stille, *etc.* [28–30], which offer the possibility of introducing a wide variety of electron accepting units and/or anchor groups for attachment of the dyads to semiconductors. Furthermore, the perfluorinated phenyl groups can easily undergo regioselective S_NAr by different nucleophiles, thereby offering an extra site for substitution. As mentioned above, the aldehyde can be used to introduce an additional benzimidazole moiety to generate a structure which can exhibit three proton transfers in conjunction with the oxidation of the phenol (an E3PT process).

Structural characterization

Figure 1 presents the downfield region of the 1H NMR spectra taken in $CDCl_3$ of compounds **6**, **7**, **12** and **13**. The sharp signal at ~14.20 ppm corresponds to the strongly deshielded phenolic proton of compounds **6**, **12** and **13**. The deshielding of these signals is due to the strong H-bond between the phenolic proton and the nitrogen lone pair of the imidazole group. This is probably due to the strong electron-withdrawing effect of the fluorine substituted porphyrin and the good electronic communication between the tetrapyrrolic macrocycle and the phenolic ring [19]. On the other hand, in compound **7** the phenolic proton resonance is shifted upfield, indicative of a weaker H-bond. As was previously reported, in $CDCl_3$ the 1H NMR spectrum of BIP, lacking substitution on the benzimidazole ring, shows a chemical shift of 13.46 ppm for the OH, similar to that of compound **7** [10]. In the case of **7** the electron-withdrawing effect of the macrocycle must be greatly diminished compared to that observed in **6**, **12** and **13**. This is most likely due to the presence of the large substituent at the *ortho* position of the *meso* phenyl group, which causes the dihedral angle between the macrocycle and the *meso* phenyl group to increase. This structural feature is expected to reduce the electronic coupling between the macrocycle and the phenol, with the ensuing increase of the phenolic pK_a in **7** compared to that of the phenol in **6**, **12** and **13**, and results in a weaker H-bond between the phenol and the N of the imidazole [14, 19].

Evidence for the formation of a H-bond between the distal NH of benzimidazole and the imine N comes from their 1H NMR spectra (see Fig. 1). When benzimidazole is not substituted, the NH chemical shift appears upfield compared to that of compounds substituted by the imino group. In a BIP lacking substitution on the benzimidazole moiety and not attached to a porphyrin, this signal appears at 9.34 ppm, similar to that observed for compounds **6** and **7** [12]. The NH chemical shift of compounds **12** and **13** is considerably downfield and this effect is attributed to the formation of a strong H-bond between the NH and the lone pair of the imino N. The NH

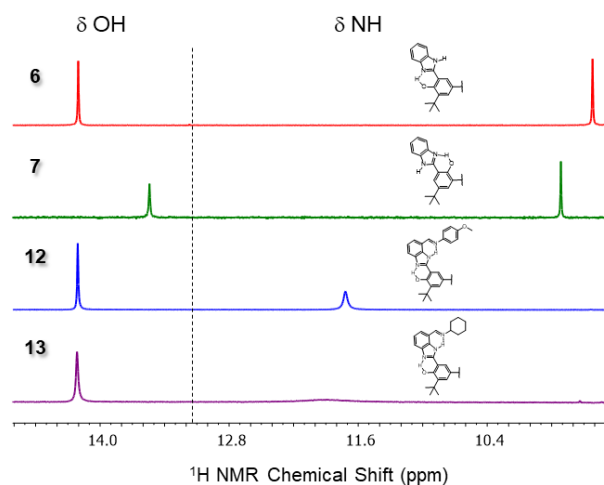


Fig. 1. Difference in chemical shift of the phenolic proton and benzimidazole NH for compounds **6**, **7**, **12** and **13** in $CDCl_3$

in compound **13** is observed as a broad band. This was previously observed in BIPs substituted at the 7-position with good proton acceptors such as amino groups and *p*-dimethylaminophenyl imines [10, 15]. Presumably, this effect is due to fast exchange of the proton between the imidazole N and the imine N on the NMR time scale.

As mentioned above, when fluorinated porphyrins such as those of Schemes 2 and 3 are used in synthetic procedures, the possibility of replacement of fluorine atoms by basic groups at the *para* position *via* S_NAr has to be considered. ^{19}F NMR spectra were used to confirm the structure of compounds **6**, **13** and **15**, indicating the stability of the fluorine substituted phenyl groups under the reaction conditions employed in this work (Figs S7, S15 and S17).

CONCLUSION

New artificial photosynthetic models of P680-Tyr_z-His190 have been designed and synthesized. The reactions and purifications have been optimized and the reported procedures resulted in good yields. The photochemically driven PCET processes in the constructs described herein require three critical prerequisites: high redox potential porphyrins, adequate electronic coupling between the porphyrin and the BIP moiety, and a well-defined H-bond network formed between the sites where the proton transfer(s) take place.

The position of the hydroxy group of the phenol attached to the *meso* position of the macrocycle must be taken into consideration because of the difference in the H-bond strength between the phenolic proton and the nitrogen lone pair of the benzimidazole in isomeric systems. The H-bond is stronger when the OH is located in the *para* position of the *meso* phenyl group.

To effectively carry out intramolecular E2PT processes, a second proton acceptor such as an imino group has been

included in the benzimidazole portion of the molecule. The synthetic route for such systems must consider the conditions necessary to prevent the loss of fluorine atoms from the pentafluorophenyl groups. It is noteworthy that the fluorine-substituted phenyl groups are stable under the conditions of the Philipps–Ladenburg reaction. Also, mild conditions were found using DIBALH as the reducing agent to convert the ester group at the 7-position of the BIP to the alcohol at -78°C . After oxidation of the alcohol the aldehyde derivative was obtained, which serves as a precursor of the molecules that can undergo the E2PT processes.

The synthesis of porphyrins requires several combinations of dipyrromethanes and aldehydes. In this work we have chosen two different halogen substituents in the *para* positions of benzaldehydes for the construction of porphyrin-based assemblies bearing electron accepting moieties and/or anchoring groups for semiconductor nanoparticles.

Transient absorption studies with excitation in the visible and detection in the IR on the molecules synthesized in the present work will provide information essential to understanding the dynamics of E1PT and E2PT processes. Specifically, we hope to determine on the femtosecond time scale the extent to which electron and proton movements are correlated in these E1PT and E2PT processes. We anticipate that this information will further define the concept of “concerted” in the context of PCET.

EXPERIMENTAL

General

The chemicals used in synthesis were purchased from Aldrich, Acros and Alfa Aesar. Solvents were purchased from VWR. Dichloromethane (CH_2Cl_2) was distilled from calcium hydride (CaH_2) and kept over molecular sieves. Thin layer chromatography (TLC) was performed with silica-gel-coated glass plates from Merck Millipore. All column chromatography purifications were conducted with Silicycle silica gel 60 (230–400 mesh). Mass spectra of each compound were obtained using a Voyager DE STR matrix-assisted laser desorption/ionization time-of-flight (MALDI-TOF) mass spectrometer. The spectra were taken in positive ion and reflector modes with *trans*, *trans*-1,4-diphenyl-1,3-butadiene as the matrix. Nuclear Magnetic Resonance (NMR) spectra were obtained with 500 and 400 MHz Bruker spectrometers at 25°C using standard pulse techniques. Deuterated chloroform (CDCl_3) was used as the solvent for the NMR samples with TMS (0.05% v/v) as the internal reference.

Synthesis

5-(Pentafluorophenyl)dipyrromethane, F_5 -DPM (1). A procedure similar to that described below was

previously reported [18]. A portion of 2,3,4,5,6-pentafluorobenzaldehyde (2 mL, 16.2 mmol) in freshly distilled pyrrole (50 mL, 720 mmol) was stirred and kept under an argon atmosphere. After 15 min, trifluoroacetic acid (TFA) (120 μL , 160 mmol) was added dropwise. The mixture was diluted after 1 h with CH_2Cl_2 (400 mL) and extracted with water, controlling the pH of the aqueous phase at around 7 using a NaOH solution. The organic layer was then dried over sodium sulfate (Na_2SO_4) and the solvent was removed under reduced pressure. The excess of pyrrole was removed under high vacuum. The light yellow oily solid was purified by column chromatography on silica gel using hexanes/15% ethyl acetate/0.5% triethylamine (TEA). The white solid was recrystallized from hexanes/ CH_2Cl_2 to afford 2.9 g of pure **1** (57% yield). ^1H NMR (400 MHz, CDCl_3): δ 5.90 (1H, br s, CH), 6.03 (2H, br s, CH), 6.16–6.18 (2H, m, CH), 6.72–6.74 (2H, m, CH), 8.12 (2H, br s, NH).

5-(3-Formyl-4-hydroxy-5-*tert*-butylphenyl-1-yl)-10,15,20-tris(2,3,4,5,6-pentafluorophenyl)porphyrin, PF_{15} -4OH (2). A procedure similar to that described below was previously reported [18]. Compound **1** (1 g, 3.2 mmol), 5-formyl-3-*tert*-butyl-2-hydroxybenzaldehyde previously synthesized in our laboratory (330 mg, 1.6 mmol) and 2,3,4,5,6-pentafluorobenzaldehyde (207 μL , 1.68 mmol) were combined in a flask and dissolved in 400 mL of chloroform/0.75% EtOH under an argon atmosphere. Boron-trifluoride etherate (BF_3OEt_2) (156 μL , 1.25 mmol) was added to the flask and the mixture was stirred at room temperature for 3 h. The resulting product was oxidized with 2,3-dichloro-5,6-dicyano-1,4-benzoquinone (DDQ) (1.45 g, 6.4 mmol) at 40°C overnight. The mixture was then filtered through a silica pad and concentrated under reduced pressure. The solid was purified by column chromatography on silica gel using a gradient of solvents from hexanes/ CH_2Cl_2 4:1 to 1:1 to afford 270 mg of pure **2** (16% yield). ^1H NMR (400 MHz, CDCl_3): δ -2.82 (2H, s, pyrrolic NH), 1.62 (9H, s, $\text{C}(\text{CH}_3)_3$), 8.23 (1H, d, $J = 2.2$ Hz, ArH), 8.41 (1H, d, $J = 2.1$ Hz, ArH), 8.85 (2H, d, $J = 4.6$ Hz, pyrrolic H), 8.88–8.91 (4H, m, pyrrolic H), 8.97 (2H, d, $J = 4.7$ Hz, pyrrolic H), 10.15 (1H, s, CHO), 12.25 (1H, s, OH). MALDI-TOF-MS m/z . calcd. for $\text{C}_{49}\text{H}_{23}\text{F}_{15}\text{N}_4\text{O}_2^+$ 984.157, experimental: 984.154 (M) $^+$.

5-(2-Hydroxy-3-formyl-5-*tert*-butylphenyl-1-yl)-10,15,20-tris(2,3,4,5,6-pentafluorophenyl)porphyrin, PF_{15} -2OH (3). The same procedure used in the synthesis of **2** was followed, using 5-(*tert*-butyl)-2-hydroxyisophthalaldehyde previously synthesized in our laboratory. The residue was then purified by column chromatography on silica gel using a gradient of hexanes/ CH_2Cl_2 3:1 to pure CH_2Cl_2 , to give 300 mg of compound **3** (65% yield). ^1H NMR (400 MHz, CDCl_3): δ -2.83 (2H, s, pyrrolic NH), 1.53 (9H, s, $\text{C}(\text{CH}_3)_3$), 8.05 (1H, d, $J = 2.5$ Hz, ArH), 8.35 (1H, d, $J = 2.4$ Hz, ArH), 8.82 (2H, d, $J = 4.7$ Hz, pyrrolic H), 8.89 (4H, br s, pyrrolic H), 8.92 (2H, d, $J = 4.7$ Hz, pyrrolic H), 10.27 (1H, s, CHO), 11.33 (1H, s, OH).

MALDI-TOF-MS *m/z.* calcd. for $C_{49}H_{23}F_{15}N_4O_2^+$ 984.157, experimental: 984.146 (M)⁺.

5-(3-Formyl-4-hydroxy-5-tert-butylphenyl-1-yl)-15-(4-iodophenyl)-10,20-bis(2,3,4,5,6-pentafluorophenyl)porphyrin, PF₁₀-4OH-PI (4). Compound **1** (1.82 g, 5.82 mmol), 5-formyl-3-tert-butyl-2-hydroxybenzaldehyde (600 mg, 2.91 mmol) and 4-iodobenzaldehyde (675 mg, 2.91 mmol) were dissolved in 740 mL of CHCl₃ containing 5.6 mL of EtOH under an argon atmosphere. BF₃OEt₂ (283 μL, 2.27 mmol) was added and the mixture was stirred at room temperature for 1 h. The resulting product was oxidized with DDQ (1.98 g, 8.73 mmol) at room temperature overnight. The mixture was then filtered through a silica pad to remove polymeric byproducts and concentrated under reduced pressure. The resulting solid was purified by column chromatography on silica gel (hexanes/CH₂Cl₂, from 3:2 to 1:4), affording the target porphyrin **4** (0.415 g, 14% yield) as a purple solid. ¹H NMR (400 MHz, CDCl₃): δ -2.84 (2H, s, pyrrolic NH), 1.62 (9H, s, C(CH₃)₃), 7.95 (2H, brt, *J* = 7.4 Hz, ArI), 8.14 (2H, d, *J* = 8.2 Hz, ArI), 8.23 (1H, d, *J* = 2.1 Hz, ArH), 8.42 (1H, d, *J* = 2.1 Hz, ArH), 8.80–8.86 (4H, brt, pyrrolic H), 8.92–8.99 (4H, brt, pyrrolic H), 10.15 (1H, s, CHO), 12.24 (1H, s, OH). MALDI-TOF-MS *m/z.* calcd. for $C_{49}H_{27}F_{10}IN_4O_2^+$ 1020.101, experimental: 1020.102 (M)⁺.

5-(3-Formyl-4-hydroxy-5-tert-butylphenyl-1-yl)-15-(4-bromophenyl)-10,20-bis(2,3,4,5,6-pentafluorophenyl)porphyrin, PF₁₀-4OH-pBr (5). Compound **1** (908 mg, 2.91 mmol), 5-formyl-3-tert-butyl-2-hydroxybenzaldehyde (300 mg, 1.45 mmol) and 4-bromobenzaldehyde (269 mg, 1.45 mmol) were dissolved in 370 mL of chloroform containing 2.8 mL of EtOH under an argon atmosphere. BF₃OEt₂ (161 μL, 1.14 mmol) was added and the mixture was stirred at room temperature for 1 h. The resulting product was oxidized with DDQ (987 mg, 4.35 mmol) at room temperature overnight. The mixture was then filtered through a silica pad to remove polymeric byproducts and concentrated under reduced pressure. The resulting solid was purified by column chromatography on silica gel using a gradient of solvents hexanes/CH₂Cl₂ from 6:4 to 2:8 to yield the target porphyrin **5** (175 mg, 14% yield) as a purple solid. ¹H NMR (400 MHz, CDCl₃) δ -2.84 (2H, s, pyrrolic NH), 1.62 (9H, s, C(CH₃)₃), 7.94 (2H, d, *J* = 8.3 Hz, ArBr), 8.09 (2H, brt, ArBr), 8.24 (1H, d, *J* = 2.1 Hz, ArH), 8.42 (1H, d, *J* = 2.1 Hz, ArH), 8.84 (4H, brt, 4H, pyrrolic H), 8.99–8.91 (4H, m, pyrrolic H), 10.15 (1H, s, CHO), 12.24 (1H, s, OH). MALDI-TOF-MS *m/z.* calcd. for $C_{49}H_{27}BrF_{10}N_4O_2^+$ 972.115, experimental: 972.153 (M)⁺.

5-(3-(Benzimidazole-2-yl)-4-hydroxy-5-tert-butylphenyl-1-yl)-10,15,20-tris(2,3,4,5,6-pentafluorophenyl)porphyrin, PF₁₅-4OHBIP (6). *o*-Phenylenediamine (12 mg, 0.11 mmol) in 5 mL of nitrobenzene was added dropwise to a solution of **2** (102 mg, 0.1 mmol) in 10 mL of nitrobenzene. The mixture was stirred and kept under an argon atmosphere. After 1 h, the reaction was refluxed

overnight at 200 °C. The solvent was removed under high vacuum and the residue was then purified by column chromatography on silica gel using hexanes/CH₂Cl₂ 4:1 to 1:1 as the eluent, to give 101 mg of **6** (93% yield). ¹H NMR (400 MHz, CDCl₃): δ -2.77 (2H, s, pyrrolic NH), 1.71 (9H, s, C(CH₃)₃), 7.25–7.29 (overlap with solvent signal, m, ArH), 7.32–7.37 (2H, m, ArH), 7.85 (1H, d, *J* = 8.1 Hz, ArH), 8.30 (2H, s, ArH), 8.85 (2H, d, *J* = 4.6 Hz, pyrrolic H), 8.89–8.93 (4H, m, pyrrolic H), 9.09 (2H, d, *J* = 4.8 Hz, pyrrolic H), 9.45 (1H, s, NH), 14.20 (1H, s, OH). ¹⁹F NMR (470 MHz, CDCl₃): δ -161.75–-161.43 (F_{meta}, m), -151.75–-151.60 (F_{para}, m), -137.00–-136.44 (F_{ortho}, m). MALDI-TOF-MS *m/z.* calcd. for $C_{55}H_{28}F_{15}N_6O^+$ 1073.208, experimental: 1073.213 (M+H)⁺.

5-(2-Hydroxy-3-(benzimidazole-2-yl)-5-tert-butylphenyl-1-yl)-10,15,20-tris(2,3,4,5,6-pentafluorophenyl)porphyrin, PF₁₅-2OHBIP (7). The same procedure used in the synthesis of **3** was followed. The residue was purified by column chromatography on silica gel using a gradient of hexanes/CH₂Cl₂ 3:1 to pure CH₂Cl₂ as the eluent, to obtain 210 mg of **7** (70% yield). ¹H NMR (400 MHz, CDCl₃): δ -2.80 (2H, s, pyrrolic NH), 1.55 (9H (+ H₂O overlap), s, C(CH₃)₃), 7.18 (2H, br s, ArH), 7.49 (2H, d, *J* = 8.4 Hz, ArH), 8.06 (1H, d, *J* = 2.3 Hz, ArH), 8.17 (1H, d, *J* = 2.3 Hz, ArH), 8.81 (2H, d, *J* = 4.6 Hz, pyrrolic H), 8.89 (4H, br s, pyrrolic H), 9.05 (2H, d, *J* = 4.7 Hz, pyrrolic H), 9.81 (1H, br s, NH), 13.55 (1H, br s, OH). MALDI-TOF-MS *m/z.* calcd. for $C_{55}H_{28}F_{15}N_6O^+$ 1073.208, experimental: 1073.236 (M + H)⁺.

5-(3-(7-Carbomethoxybenzimidazole-2-yl)-4-hydroxy-5-tert-butylphenyl-1-yl)-10,15,20-tris(2,3,4,5,6-pentafluorophenyl)porphyrin, PF₁₅-BIPCOOME (8). The same procedure used in the synthesis of **6** was followed, using methyl 2,3-diaminobenzoate (16.1 mg, 0.097 mmol) dissolved in 5 mL nitrobenzene. The solution of 2,3-diaminobenzoate was added dropwise to a solution of **2** (95.3 mg, 0.097 mmol) in 10 mL of nitrobenzene. The residue was then purified by column chromatography on silica gel using hexanes/CH₂Cl₂ (8:2 to 1:1) as eluent, to give 80.8 mg of **8** (74% yield). ¹H NMR (500 MHz, CDCl₃): δ -2.82 (2H, s, pyrrolic NH), 1.69 (9H, s, C(CH₃)₃), 3.74 (3H, s, COOCH₃), 7.04 (1H, t, *J* = 7.9 Hz, ArH), 7.64 (1H, d, *J* = 7.6 Hz, CH), 7.75 (1H, d, *J* = 8.2 Hz, ArH), 8.25 (1H, d, *J* = 2.1 Hz, ArH), 8.39 (1H, d, *J* = 2.1 Hz, ArH), 8.84 (2H, d, *J* = 4.4 Hz, pyrrolic H), 8.89–8.93 (4H, m, pyrrolic H), 9.03 (2H, d, *J* = 4.6 Hz, pyrrolic H), 10.72 (1H, s, NH), 13.99 (1H, s, OH). MALDI-TOF-MS *m/z.* calcd. for $C_{57}H_{30}F_{15}N_6O_3^+$ 1131.214, experimental: 1131.210 (M + H)⁺.

5-(3-(7-Carbomethoxybenzimidazole-2-yl)-4-hydroxy-5-tert-butylphenyl-1-yl)-15-(4-iodophenyl)-10,20-bis(2,3,4,5,6-pentafluorophenyl)porphyrin, PF₁₀-PI-BIPCOOME (9). Methyl 2,3-diaminobenzoate (36 mg, 0.22 mmol) in 10 mL of nitrobenzene was added dropwise to a solution of **4** (200 mg, 0.196 mmol) in 20 mL of nitrobenzene. The mixture was stirred and purged with argon for 30 min.

The reaction was refluxed at 200 °C for 16 h under an argon atmosphere. The solvent was removed under high vacuum. The residue was then purified by column chromatography on silica gel using hexanes/CH₂Cl₂ from 7:3 to 6:4 as eluent, to give 193 mg of **4** (84% yield) as a purple solid. ¹H NMR (500 MHz, CDCl₃): δ -2.81 (2H, s, pyrrolic NH), 1.69 (9H, s, C(CH₃)₃), 3.77 (3H, s, -OMe), 7.32 (1H, t, *J* = 8.0 Hz, ArBIP), 7.85 (1H, d, *J* = 7.6 Hz, ArBIP), 8.02–7.94 (3H, m, ArI+ArBIP), 8.14 (2H, d, *J* = 8.1 Hz, ArI), 8.28 (1H, d, *J* = 2.1 Hz, ArOH), 8.38 (1H, d, *J* = 2.1 Hz, ArOH), 8.84 (4H, brt, pyrrolic H), 8.95 (2H, d, *J* = 4.7 Hz, pyrrolic H), 9.04 (2H, d, *J* = 4.7 Hz, pyrrolic H), 10.73 (1H, s, NH), 13.98 (1H, s, OH). MALDI-TOF-MS *m/z*. calcd. for C₅₇H₃₄F₁₀IN₆O₃⁺ 1167.157, experimental: 1167.114 (M + H)⁺.

5-(3-(7-Hydroxymethylbenzimidazole-2-yl)-4-hydroxy-5-tert-butylphenyl-1-yl)-10,15,20-tris(2,3,4,5,6-pentafluorophenyl)porphyrin, PF₁₅-BIPCH₂OH (10). Compound **8** (73.4 mg, 0.0649 mmol) in 4 mL of dry CH₂Cl₂ was stirred at -78 °C under argon. A solution of 25% DIBALH (260 μL, 0.3892 mmol) in toluene was added dropwise and the reaction was stirred for 4 h. To quench the reaction, 8 mL of 3M HCl solution (kept cold) was added and the mixture was stirred overnight. The resulting mixture was extracted 3 times with CH₂Cl₂, controlling the pH of the aqueous phase at around 7 using a sodium bicarbonate (NaHCO₃) solution. The organic layer was then dried over Na₂SO₄ and the solvent was removed under reduced pressure. The solid was purified by column chromatography on silica gel using a gradient of hexanes/CH₂Cl₂ 1:1 to CH₂Cl₂ as the eluent, to give 183 mg of **10** (70% yield). ¹H NMR (500 MHz, CDCl₃): δ -2.88 (2H, s, pyrrolic NH), 1.68 (9H, s, C(CH₃)₃), 4.80 (2H, s, CH₂), 6.73 (1H, d, *J* = 6.6 Hz, ArH), 6.91 (1H, t, *J* = 7.6 Hz, ArH), 7.42 (1H, d, *J* = 8.1 Hz, ArH), 8.21 (1H, d, *J* = 2.0 Hz, ArH), 8.32 (1H, d, *J* = 2.1 Hz, ArH), 8.84 (2H, d, *J* = 4.2 Hz, pyrrolic H), 8.88–8.92 (4H, m, pyrrolic H), 9.04 (2H, d, *J* = 4.5 Hz, pyrrolic H), 10.16 (1H, s, NH), 14.20 (1H, s, ArOH); isomeric species were detected in the spectrum. MALDI-TOF-MS *m/z*. calcd. for C₅₆H₃₀F₁₅N₆O₂⁺ 1103.218, experimental: 1103.224 (M + H)⁺.

5-(3-(7-Formylbenzimidazole-2-yl)-4-hydroxy-5-tert-butylphenyl-1-yl)-10,15,20-tris(2,3,4,5,6-pentafluorophenyl)porphyrin, PF₁₅-BIPCHO (11). A procedure similar to that described below was previously reported [15]. Compound **10** (30.1 mg, 0.027 mmol) was dissolved in 15 mL of dry CH₂Cl₂, and the solution was stirred under argon. Activated MnO₂ was added carefully at room temperature, and the oxidation reaction was followed by thin-layer chromatography (TLC). After completion, the reaction mixture was filtered through a pad of celite and the residue was washed with CH₂Cl₂. The solvent was removed under reduced pressure. The solid was purified by column chromatography on silica gel using hexanes/CH₂Cl₂ 3:2 as the eluent to afford 21.9 mg of pure **11** (74% yield). ¹H NMR (500 MHz, CDCl₃): δ -3.26 (2H, s,

pyrrolic NH), 1.64 (9H, s, C(CH₃)₃), 5.59 (2H, s, ArH), 6.45 (1H, br d, *J* = 5.5 Hz, ArH), 8.06 (1H, d, *J* = 1.9 Hz, ArH), 8.52 (1H, d, *J* = 1.9 Hz, ArH), 8.62 (1H, s, CHO), 8.78 (2H, br s, pyrrolic H), 8.88 (2H, d, *J* = 4.3 Hz, pyrrolic H), 8.95–8.98 (4H, m, pyrrolic H), 10.76 (1H, s, NH), 13.65 (1H, s, OH). MALDI-TOF-MS *m/z*. calcd. for C₅₆H₂₈F₁₅N₆O₂⁺ 1101.203, experimental: 1101.203 (M + H)⁺.

5-(3-(7-(4-Methoxyphenyliminomethyl)-benzimidazole-2-yl)-4-hydroxy-5-tert-butylphenyl-1-yl)-10,15,20-tris(2,3,4,5,6-pentafluorophenyl)porphyrin, PF₁₅-BIP-Ph^{OMe}imine (12). A procedure similar to that described below was previously reported [15, 27]. A solution of **11** (22 mg, 0.020 mmol) and *p*-anisidine (2.5 mg, 0.020 mmol) with 4 Å molecular sieves in 2 mL of dry CH₂Cl₂ was stirred and kept under an argon atmosphere at room temperature. After 15 min, pyrrolidine (0.002 mmol) was added. After 24 h, the reaction mixture was filtered and the molecular sieves washed several times with dry CH₂Cl₂. The solvent was removed under reduced pressure to afford 20 mg of pure **12** (83% yield). ¹H NMR (500 MHz, CDCl₃): δ -2.81 (2H, s, pyrrolic NH), 1.69 (9H, s, C(CH₃)₃), 3.41 (3H, s, OCH₃), 6.38–6.42 (2H, m, ArH), 6.80–6.84 (2H, m, ArH), 7.35 (overlap with solvent, br s, ArH), 7.85 (1H, br s, ArH), 8.26 (1H, d, *J* = 2.0 Hz, ArH), 8.33 (1H, d, *J* = 2.1 Hz, ArH), 8.53 (1H, br s, CH=N), 8.84 (2H, d, *J* = 4.5 Hz, pyrrolic H), 8.87–8.90 (4H, m, pyrrolic H), 9.09 (2H, d, *J* = 4.6 Hz, pyrrolic H), 11.73 (1H, s, NH), 14.20 (1H, s, OH). MALDI-TOF-MS *m/z*. calcd. for C₆₃H₃₅F₁₅N₇O₂⁺ 1206.260, experimental: 1206.205 (M + H)⁺.

5-(7-(N-Cyclohexyliminebenzimidazole-2-yl)-4-hydroxy-5-tert-butylphenyl-1-yl)-10,15,20-tris(2,3,4,5,6-pentafluorophenyl)porphyrin, PF₁₅-BIP-Cyimine (13). This reaction uses the same conditions as the previous reaction but employs cyclohexylamine. The solvent was removed under reduced pressure to afford 25 mg of the desired pure compound **13** (87% yield). ¹H NMR (500 MHz, CDCl₃): δ -2.75 (2H, s, pyrrolic NH), 0.87–0.95 (3H, m, cy ring), 1.05–1.12 (2H, m, cy ring), 1.26–1.32 (3H, m, cy ring), 1.43–1.46 (2H, m, cy ring), 1.71 (9H, s, C(CH₃)₃), 3.09–3.14 (1H, m, CH-N), 7.38 (2H, d, *J* = 4.2 Hz, ArH), 7.88–7.91 (1H, m, ArH), 8.28 (1H, d, *J* = 2.0 Hz, ArH), 8.33 (1H, d, *J* = 2.1 Hz, ArH), 8.42 (1H, s, CH=N), 8.87 (2H, d, *J* = 4.5 Hz, pyrrolic H), 8.89–8.92 (4H, m, pyrrolic H), 9.17 (2H, d, *J* = 4.6 Hz, pyrrolic H), 11.92 (1H, br s, NH), 14.22 (1H, s, OH). ¹⁹F NMR (470 MHz, CDCl₃): δ -161.80 (F_{meta}, td), -161.66– -161.49 (F_{meta}, m), -151.84– -151.66 (F_{para}, m), -136.92– -136.47 (F_{ortho}, m). MALDI-TOF-MS *m/z*. calcd. for C₆₂H₃₉F₁₅N₇O⁺ 1182.297, experimental: 1182.205 (M + H)⁺.

5-(3-(7-Hydroxymethylbenzimidazole-2-yl)-4-hydroxy-5-tert-butylphenyl-1-yl)-15-(4-iodophenyl)-10,20-bis(2,3,4,5,6-pentafluorophenyl)porphyrin, PF₁₀-pI-BIPCH₂OH (14). A solution of compound **9** (75 mg, 65 μmol) in 5 mL of dry CH₂Cl₂ was stirred at -78 °C under an

argon atmosphere. A solution of 25% DIBALH (267 μL , 390 μmol) in toluene was added dropwise and the reaction was stirred for 4 h. After that, 8 mL of 3M HCl solution was added (kept cold) to quench the reaction. The reaction mixture was allowed to reach room temperature and stirred overnight under an argon atmosphere. The mixture was poured into 25 mL of water and 20 mL of CH_2Cl_2 . Then it was extracted 3 times with CH_2Cl_2 , controlling the pH of the aqueous phase at around 7 using a sodium bicarbonate (NaHCO_3) solution. The organic layer was then washed with water and dried over Na_2SO_4 and the solvent was removed under reduced pressure. The solid was purified by column chromatography on silica gel using hexanes/ CH_2Cl_2 7:3 as the eluent, to give **14** (65 mg, 89%). At least two isomeric species were detected in the ^1H NMR spectrum. MALDI-TOF-MS m/z . calcd. for $\text{C}_{56}\text{H}_{34}\text{F}_{10}\text{IN}_6\text{O}_2^+$ 1139.162, experimental: 1139.145 (M + H) $^+$.

5-(3-(7-Formylbenzimidazole-2-yl)-4-hydroxy-5-tert-butylphenyl-1-yl)-15-(4-iodophenyl)-10,20-bis(2,3,4,5,6-pentafluorophenyl)porphyrin, PF₁₀-pI-BIPCHO (15). Compound **14** (55 mg, 48 μmol) was dissolved in 15 mL of dry CH_2Cl_2 , and the solution was stirred under argon. Activated MnO_2 (140 mg, 1.61 mmol) was added carefully at room temperature, and the oxidation reaction was followed by TLC. After completion (4 h), the reaction mixture was concentrated under reduced pressure and purified by column chromatography on silica gel using hexanes/ CH_2Cl_2 1:1 to afford 50 mg of pure **15** (91% yield). ^1H NMR (500 MHz, CDCl_3): δ -2.94 (2H, s, pyrrolic NH), 1.66 (9H, s, $\text{C}(\text{CH}_3)_3$), 6.49 (1H, t, $J = 7.7$ Hz, ArBIP), 6.59 (1H, d, $J = 7.1$ Hz, ArBIP), 7.38 (1H, d, $J = 8.1$ Hz, ArBIP), 7.97 (1H, d, $J = 7.8$ Hz, ArI), 8.02 (1H, d, $J = 7.8$ Hz, ArI), 8.16 (2H, brt, ArI), 8.21 (1H, d, $J = 1.8$ Hz, ArH), 8.44 (1H, d, $J = 1.8$ Hz, ArH), 8.82 (2H, d, $J = 4.4$ Hz, pyrrolic H), 8.86 (2H, d, $J = 4.4$ Hz, pyrrolic H), 8.97 (4H, brt, pyrrolic H), 9.31 (1H, s, CHO), 10.99 (1H, s, NH), 13.75 (1H, s, OH). ^{19}F NMR (470 MHz, CDCl_3): δ -162.04–-161.69 (F_{meta} , m), -152.22 (F_{para} , t, $J = 20.8$ Hz), -136.79 (F_{ortho} , dd, $J = 24.1, 7.3$ Hz). MALDI-TOF-MS m/z . calcd. for $\text{C}_{56}\text{H}_{32}\text{F}_{10}\text{IN}_6\text{O}_2^+$ 1137.146, experimental: 1137.107 (M + H) $^+$.

Acknowledgments

This research was supported by the U.S. Department of Energy, Office of Science, Office of Basic Energy Sciences, under Award DE-FG02-03ER15393.

Supporting information

The synthetic route of compound **15** and, ^1H NMR characterization for all the compounds and ^{19}F NMR for compounds **6**, **13** and **15** are given in the supplementary material. This material is available free of charge via the Internet at <http://www.worldscinet.com/jpp/jpp.shtml>.

REFERENCES

- Tommos C and Babcock GT. *Biochim. Biophys. Acta - Bioenerg.* 2000; **1458**: 199–219.
- Barry BA and Babcock GT. *Proc. Natl. Acad. Sci.* 1987; **84**: 7099–7103.
- Yano J and Yachandra V. *Chem. Rev.* 2014; **114**: 4175–4205.
- Umena Y, Kawakami K, Shen J-R and Kamiya N. *Nature* 2011; **473**: 55–60.
- Suga M, Akita F, Sugahara M, Kubo M, Nakajima Y, Nakane T, Yamashita K, Umena Y, Nakabayashi M, Yamane T, Nakano T, Suzuki M, Masuda T, Inoue S, Kimura T, Nomura T, Yonekura S, Yu L-J, Sakamoto T, Motomura T, Chen J-H, Kato Y, Noguchi T, Tono K, Joti Y, Kameshima T, Hatsui T, Nango E, Tanaka R, Naitow H, Matsuura Y, Yamashita A, Yamamoto M, Nureki O, Yabashi M, Ishikawa T, Iwata S and Shen J-R. *Nature* 2017; **543**: 131–135.
- Rappaport F, Boussac A, Force DA, Peloquin J, Brynda M, Sugiura M, Un S, Britt RD and Diner BA. *J. Am. Chem. Soc.* 2009; **131**: 4425–4433.
- Blankenship RE. *Molecular Mechanisms of Photosynthesis*. Second Ed. Oxford, UK, Hoboken, NJ, USA: Wiley Blackwell; 2014.
- Keough JM, Jenson DL, Zuniga AN and Barry BA. *J. Am. Chem. Soc.* 2011; **133**: 11084–11087.
- Vogt L, Vinyard DJ, Khan S and Brudvig GW. *Curr. Opin. Chem. Biol.* 2015; **25**: 152–158.
- Huynh MT, Mora SJ, Villalba M, Tejada-Ferrari ME, Liddell PA, Cherry BR, Teillout A-L, Machan CW, Kubiak CP, Gust D, Moore TA, Hammes-Schiffer S and Moore AL. *ACS Cent. Sci.* 2017; **3**: 372–380.
- Moore GF, Hambourger M, Gervaldo M, Poluektov OG, Rajh T, Gust D, Moore TA and Moore AL. *J. Am. Chem. Soc.* 2008; **130**: 10466–10467.
- Moore GF, Hambourger M, Kodis G, Michl W, Gust D, Moore TA and Moore AL. *J. Phys. Chem. B* 2010; **114**: 14450–14457.
- Moore TA, Gust D, Hatlevig S, Moore AL, Makings LR, Pesski PJ, De Schryver FC, van Der Auwer-aer M, Lexa D, Bensasson R V and Rougée M. *Isr. J. Chem.* 1988; **28**: 87–95.
- Markle TF, Rhile IJ, DiPasquale AG and Mayer JM. *Proc. Natl. Acad. Sci.* 2008; **105**: 8185–8190.
- Odella E, Mora SJ, Wadsworth BL, Huynh MT, Goings JJ, Liddell PA, Groy TL, Gervaldo M, Sereno LE, Gust D, Moore TA, Moore GF, Hammes-Schiffer S and Moore AL. *J. Am. Chem. Soc.* 2018; **140**: 15450–15460.
- Moore GF, Konezny SJ, Song H, Milot RL, Blake-more JD, Lee ML, Batista VS, Schmuttenmaer CA, Crabtree RH and Brudvig GW. *J. Phys. Chem. C* 2012; **116**: 4892–4902.
- Zhao Y, Swierk JR, Megiatto JD, Sherman B, Youngblood WJ, Qin D, Lentz DM, Moore AL,

- Moore TA, Gust D and Mallouk TE. *Proc. Natl. Acad. Sci.* 2012; **109**: 15612–15616.
18. Megiatto JD, Antoniuk-Pablant A, Sherman BD, Kodis G, Gervaldo M, Moore TA, Moore AL and Gust D. *Proc. Natl. Acad. Sci.* 2012; **109**: 15578–15583.
 19. Megiatto Jr JD, Méndez-Hernández DD, Tejada-Ferrari ME, Teillout A-L, Llansola-Portolés MJ, Kodis G, Poluektov OG, Rajh T, Mujica V, Groy TL, Gust D, Moore TA and Moore AL. *Nat. Chem.* 2014; **6**: 423–428.
 20. Llansola-Portoles M, Palacios R, Kodis G, Jackson D, Megiatto J, L. Moore A, Moore T and Gust D. *Eur. Photochem. Assoc. Newsletters* 2013; **84**: 98–105.
 21. Lee C-H and Lindsey JS. *Tetrahedron* 1994; **50**: 11427–11440.
 22. Geier GR and Lindsey JS. *Tetrahedron* 2004; **60**: 11435–11444.
 23. Materna KL, Jiang J, Crabtree RH and Brudvig GW. *ACS Appl. Mater. Interfaces* 2019; **11**: 5602–5609.
 24. Jiang J, Spies JA, Swierk JR, Matula AJ, Regan KP, Romano N, Brennan BJ, Crabtree RH, Batista VS, Schmuttenmaer CA and Brudvig GW. *J. Phys. Chem. C* 2018; **122**: 13529–13539.
 25. Brennan BJ, Gust D and Brudvig GW. *Tetrahedron Lett.* 2014; **55**: 1062–1064.
 26. Bhupathiraju NVSDK, Rizvi W, Batteas JD and Drain CM. *Org. Biomol. Chem.* 2016; **14**: 389–408.
 27. Morales S, Guijarro FG, García Ruano JL and Cid MB. *J. Am. Chem. Soc.* 2014; **136**: 1082–1089.
 28. Chinchilla R and Nájera C. *Chem. Rev.* 2007; **107**: 874–922.
 29. Hyslop AG, Kellett MA, Iovine PM and Therien MJ. *J. Am. Chem. Soc.* 1998; **120**: 12676–12677.
 30. Vaz B, Alvarez R, Nieto M, Paniello AI and de Lera AR. *Tetrahedron Lett.* 2001; **42**: 7409–7412.